UCRL-JC-134595
PREPRINT

Proton Radiography as a Means of Material Characterization

M.B. Aufderheide III, H-S. Park, E.P. Hartouni, P.D. Barnes, D.M. Wright, R.M. Bionta, J.D. Zumbro and C.L. Morris

This paper was prepared for submittal to the
Nondestructive Characterization of Materials IX
Sydney, Australia
June 28-July 2, 1999

June 23, 1999

Lawrence Livermore National Laboratory

Proton Radiography As a Means of Material Characterization

Maurice B. Aufderheide III[*], Hye-Sook Park[*], Edward P. Hartouni[*], Peter D. Barnes[*], Douglas M. Wright[*], Richard M. Bionta[*], John D. Zumbro[#], and Christopher L. Morris[#]

[*]*Lawrence Livermore National Laboratory,* [#]*Los Alamos National Laboratory*

Abstract. We describe how protons with energies of 800 MeV or greater can be used as radiographic probes for material characterization. A feature which distinguishes protons from x-rays is their charge, which results in multiple Coulomb scattering effects in proton radiographs. Magnetic lensing can ameliorate these effects and even allow mixed substances to be disentangled. We illustrate some of these effects using 800 MeV protons radiographs of a composite step wedge composed of Aluminum, Foam, and Graphite. We discuss how proton radiographs must be manipulated in order to use standard tomographic reconstruction algorithms. We conclude with a brief description of an upcoming experiment, which will be performed at Brookhaven National Laboratory at 25 GeV.

MOTIVATION

One frontier of nondestructive evaluation is the use of tomography on thick objects. For such objects, x-rays become a problematic probe because they are attenuated so severely. This effect is partially offset if higher energy gamma rays are used, but only until the "valley" of the total photon attenuation curve is reached at roughly 1-5 MeV. For photons above this energy, pair production causes attenuation to increase again, particularly for high-Z materials. Increasing the source dose becomes a counterproductive solution because gamma rays are not just attenuated by thick objects. Compton scattering, secondary bremsstrahlung, and pair production produce a great deal of scattered radiation, which can overwhelm the direct signal needed for tomographic reconstruction.

In such cases, a more penetrating form of radiation would be useful. Higher energy hadrons, such as neutrons, can be a very effective alternative to gamma radiography. However, neutrons also suffer a great deal of scattering in thick objects and they are more difficult to control as sources. In particular, for dynamic applications in which an extremely brief (<100 ns) and intense radiation pulse is required to capture rapidly evolving features, neutrons are prohibitively expensive.

This quest for intense, fast, controllable, and extremely penetrating radiation has led groups at Livermore and Los Alamos National Labs to consider high-energy (10 GeV - ~100 GeV) protons as a radiographic probe for dynamic, thick radiography[1]. High-energy protons are not a perfect radiographic probe for this application either. Although scattering processes at these energies have been estimated to be less than a 1% effect, high-energy proton attenuation processes are more complex than the Beers-law attenuation of gamma rays. In particular, because protons are charged, they experience multiple Coulomb scattering, which results in blurred images. This blurring of images is one reason that tomography and radiography with protons was largely abandoned twenty years ago[2], although see the work of Schneider and Pedroni[3]. Interestingly, the solution to these issues can aid in material characterization.

In this paper, we will briefly discuss high-energy protons as a radiographic and tomographic probe. In the next section, we describe the physics of proton radiography. In the third section, we illustrate these points by analyzing and inferring some material properties from step wedges, using 800 MeV protons at the Los Alamos Neutron Science Center (LANSCE). In the fourth section, we discuss how tomographic reconstruction is performed with protons. In the last section, we conclude with a discussion of future work.

PHYSICS OF PROTON RADIOGRAPHY

Consider a pencil beam of protons entering a slab of finite thickness. As the protons pass through the material, they undergo nuclear reactions with relatively low probability and have many Coulomb scatters off electrons and nuclei in the material. As a result of the Coulomb scatters, the beam spreads in both position and angle. Thus, after the beam exits the material, it has been attenuated by the nuclear reactions (in a manner analogous to x-ray attenuation) but also blurred in position and angle. The beam also loses energy according to the Bethe-Bloch formula, but this is a relatively small effect (a few percent), so we will not discuss it in this paper.

Almost sixty years ago, Fermi derived an approximate treatment for multiple Coulomb scattering, in the context of cosmic rays[4]. If one assumes that the incident protons are energetic enough that only small angle scattering occurs, it is possible to derive a transport equation for the distribution function of the scattered protons:

$$\frac{\partial P}{\partial x} = -\theta_y \frac{\partial P}{\partial y} + \frac{\theta_0^2}{2x} \frac{\partial^2 P}{\partial \theta_y^{\,2}} \qquad (1)$$

where $P(x,y,\theta_y)$ is the distribution function, x is the target thickness, y is the lateral displacement, θ_y is the angular displacement, and θ_0 is the angular variance of the scattering. This expression is derived in a manner similar to the photon or neutron transport equations, except that the small angle approximation of Coulomb scattering is employed. The angular variance can be approximated by

$$\theta_0 = \frac{13.6\text{MeV}}{\beta pc}\sqrt{\int\frac{\rho dl}{X_0}} \tag{2}$$

where β is v/c of the protons, $\boldsymbol{p}$ is the proton momentum, ρ is the density of the material, and X_0 is the radiation length of the material. For the proton energies of interest here, the typical angular variance is on the order of 10 *milli*Radians (hereafter mRad).

The closed, analytic solution to this transport equation is a mixed Gaussian in $\boldsymbol{y}$ and θ_y, which demonstrates Coulomb scattering blur in both position and angle. For more details on Coulomb scattering see Börgers and Larsen[5] and the references therein. This blurring has no analog in x-ray imaging and badly compromises the quality of the resulting proton radiograph. This effect was one reason why x-rays have been preferred over protons for radiography.

Several years ago, researchers at Los Alamos realized that magnetic lenses could be used to focus these blurred images, correcting the effect of Coulomb blur. Indeed, if the right set of paired quadrupole doublets were chosen, Mottershead and Zumbro demostrated[6] that it is possible to sort the scattered beam in terms of how it has been scattered. That is, at some point in the lenses, there is a location where the protons are sorted by the magnitude of their scattering. At the center of this angular imaging plane are protons with little or no scattering, while the most scattered protons are at the largest radius. After exiting this lens, the protons are focused in the spatial plane. If one places a collimator at this intermediate angular imaging plane, it is possible to apply "angular cuts" to the proton beam, removing part of the scattered beam. In such a case, the attenuation of the proton beam has the following form:

$$\frac{I}{I_o} = \text{Exp}\left[-\int\mu\rho\text{dl}\right]\times\left\{1-\text{Exp}\left[-\frac{\theta_{cut}^2}{2\theta_0^2}\right]\right\} \tag{3}$$

where I_o is incident beam intensity, μ is the mass absorption coefficient due to nuclear reactions, and θ_{cut} is the angular cut introduced by the collimator. The first term in the attenuation is the nuclear attenuation and is analogous to x-ray attenuation processes, but the second term is due to angular attenuation and makes proton radiography unique. Angular attenuation allows another way of distinguishing material properties. Unfortunately, with only one of these images, proton radiographs are more difficult to interpret than x-ray images, because there is more physics to disentangle.

If one cascades two sets of these quadrupole doublets, with the first angular collimator followed by a tighter angular collimator in the second set of lenses, one obtains two simultaneous, unique radiographs of the same object. Each image is unique because a different angular cut will have been used. If one ratios the images, the nuclear attenuation term cancels out, leaving a nonlinear equation in θ_0 to solve, pixel by pixel.

Once one solves for θ_0, it is possible to divide out the angular attenuation from each image and also obtain the nuclear attenuation in the radiographs. As a result, with these two images, it is possible to obtain projections of nuclear attenuation length *and* radiation length, simultaneously. One can then use each of these data sets in a standard tomographic reconstruction code, obtaining two reconstructions of the the same object.

APPLICATION TO STEP WEDGES

As an example of this physics, in Figure 1 we show proton radiographs taken at the Los Alamos Neutron Science Center (LANSCE) using 800 MeV protons. This energy is not high enough to radiograph thick objects, but it is useful for thin objects such as thin layers of metal, biological specimens, and high explosives. In Figure 1 a composite step wedge composed of Aluminum, Graphite, and Foam have been radiographed using angular cuts of 20 mRad and 10 mRad. Fuji CT imaging plates have been used as the detection medium. It was hoped that we would be able to show results using CCD cameras under development at LLNL, but the LANSCE schedule has not allowed us to perform these experiments yet. We hope to get beam time soon.

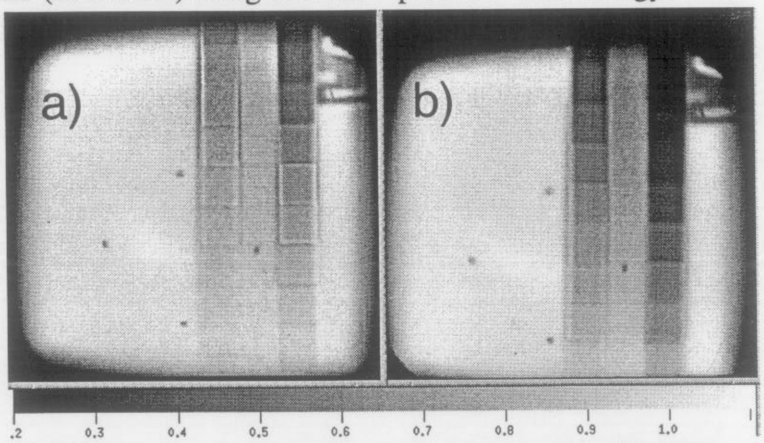

FIGURE 1: Proton radiographs of step wedges using 800 MeV protons with a) 20 and b) 10 milliradian angular cuts. The units of the grayscale are I/I_o. In each image the left wedge is Graphite, the middle wedge is CH Foam, and the right wedge is Aluminum. The four specks near the center of each image are fiducials.

The same grayscale map has been used for rendering intensity and the greater attenuation from the 10 mRad cut is apparent. The gaussian beam profile has already been divided out of the image. Each step is an increase of half an inch, starting with half-inch thickness on the bottom and ending with a 4-inch thick step at the top. The quadrupole lenses determine the field of view of the radiograph.

We have extracted average values for the attenuation over each step in both radiographs, inverted the ratio of intensities, and solved for $\int \mu\rho\, dl$ and $\int \rho / X_o\, dl$. In Figure 2, we plot these as a function of wedge thickness. We also show the fits to the data. The slope of each line gives us the nuclear mass absorption coefficient and the radiation length for each material, after we have divided out the material density. As can be seen in the figure, the values for the thickest step are compromised by the fact that they are on the edge of the field of view. We have thus not used them in our fit.

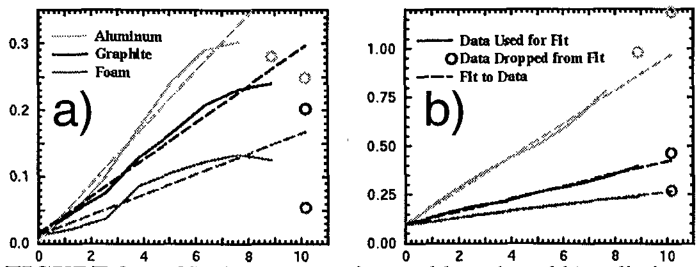

FIGURE 2: a) Nuclear attenuation pathlength and b) radiation length as functions as wedge thickness in cm.

In Table 1 we show the values obtained from these fits. The statistical uncertainties in the μ values are 4%, while the statistical uncertainties in the X_o values are 6-8%. The foam has the greatest uncertainty because it is so tenuous. Systematic uncertainties are difficult to estimate and are the subject of intensive work at present. The radiation length values inferred here are reasonable, but the μ values are difficult to verify because they are fairly energy dependent in the 800 MeV range.

TABLE 1: Results of Fits to Step Wedge Data.

Material	Density (g/cm^3)	μ(g/cm^2)	X_o(cm^2/g)
Aluminum	2.707	0.0157	31.8
Graphite	1.707	0.0162	53.1
Foam	0.922	0.0165	55.6

TOMOGRAPHIC CONSIDERATIONS

If simultaneous radiographs using two angular cuts are taken, it is possible to invert the images, obtaining a nuclear pathlength image and a radiation length image. Each of these images is in the proper format for traditional tomographic algorithms. After a tomographic reconstruction is performed, maps of the object are obtained in units of $\mu\rho$ and ρ/X_o. Thus we have two images containing a density map of the object, if μ and X_o have been measured as above and thus can be divided out.

If one is studying a region in which two substances are mixed, such as fuel and air in an engine piston, this redundancy can be used to solve for the density of each substance. In each voxel of the reconstruction,

$$\mu_1\rho_1 + \mu_2\rho_2 = \mu\rho \qquad \text{and} \qquad \frac{\rho_1}{X_1} + \frac{\rho_2}{X_2} = \frac{\rho}{X}, \tag{4}$$

where the quantities on the right of each equation are experimentally determined by inverting the ratio of the images and reconstructing, and μ_1, μ_2, X_1, and X_2 are measured using step wedges of some kind. We are exploring this capability.

CONCLUSIONS AND FUTURE WORK

This paper has been a short introduction to the physics of high energy proton radiography. We have illustrated some of the physics using data taken at LANSCE on relatively thin objects. Experiments at LANSCE are useful for testing some aspects of proton radiography, but for studying the potential of protons for doing thick object radiography, higher energy (>10 GeV) beams are needed.

This summer, we will take part in experiment E933 at Brookhaven National Laboratory, which will use 25 GeV beams to radiograph some thicker objects. The goal of the experiment is to learn what is necessary for making 1% density estimates in tomographic reconstructions of proton radiographs. Step wedges will be used to determine μs and X_os for materials of interest. Some simple objects will be radiographed and tomographically reconstructed. CCD cameras coupled to scintillators will be tested as imaging detectors. We also will study systematic effects such as resolution limits for the lensing system and sources and magnitude of various backgrounds. We eagerly await the results of these experiments.

ACKNOWLEDGMENTS

This work has been supported at Lawrence Livermore National Laboratory and Los Alamos National Laboratory by the US Dept. of Energy under Contracts W-7405-ENG-48 and Contracts W-7405-ENG-36, respectively. Work at LLNL has been funded through the LLNL proton radiography LDRD 97-ERD-058.

REFERENCES

[1] Ziock, H. J., *et al.*, "The Proton Radiography Concept", *Proceedings of the Third International Symposium on Development and Application of Semiconductor Tracking Detectors*, Melbourne, 1997, to appear in *NIM*. Los Alamos Report LA-UR-98-1368, 1998.

[2] Hanson, K. M., *et al.*, *Phys. Med. Biol.* **26**/6, 965-983 (1981), and Hanson, K. M., *et al.*, *Phys. Med. Biol.* **27**/1, 25-36 (1982).

[3] Schneider, U., and Pedroni, E., *Med. Phys.* **21**(11), 1657-1663 (1994), and Schneider, U., and Pedroni, E., *Med. Phys.* **22**(4), 353-363 (1995).

[4] Fermi, E., cited by B. Rossi and K. Griesen in *Rev. Mod. Phys.*, **13**, 265 (1941) and Eyges, L., *Phys. Rev.* **74**, 1534 (1948).

[5] Börgers, C., and Larsen, E. W., *Nucl. Sci. and Eng.*, **123**, 343 (1996).

[6] Mottershead, C. T., and Zumbro, J. D., "Magnetic Optics for Proton Radiography", in *Proceedings of the 1997 Particle Accelerator Conference*, Vancouver, B.C. (in press).